Analysis of dual laser Thomson scattering signals on W7-X

F.A. D'Isa,[a,*] **E. Pasch,**[b] **M.N.A. Beurskens,**[b] **K.J. Brunner,**[b] **G. Fuchert,**[b]
R. Pasqualotto,[a,c] **L. Giudicotti**[a] **and the W7-X team**[b]

[a]*Consorzio RFX (CNR, ENEA, INFN, Università di Padova, Acciaierie Venete SpA),*
  Corso Stati Uniti 4, 35127 Padova, Italy

[b]*Max Planck Institute for Plasma Physics,*
  Wendelsteinstr. 1, 17491 Greifswald, Germany

[c]*Istituto per la Scienza e la Tecnologia dei Plasmi, CNR,*
  Corso Stati Uniti 4, 35127 Padova, Italy

  E-mail: federico.disa@igi.cnr.it

ABSTRACT: A dual laser Thomson scattering has been developed at W7-X: a unique system employing, in combination with a 1064 nm laser, a 1319 nm Nd:YAG laser. Dual-laser Thomson scattering (DLTS) is an advanced diagnostic technique in which two laser pulses of different wavelengths are sent to the plasma with a very short time delay and the two scattered signals are separately and independently measured with the same set of polychromators. For the first time during OP2.1, a dual laser Thomson scattering system was operated stably during the entire experimental campaign. In this work, the dual-wavelength signals recorded in several W7-X discharges are analyzed with different methods and the resulting electron temperature profiles and the experimental errors are discussed, with the aim of identifying the capabilities of this technique.

---

*Corresponding author.

1 Introduction

The dual-wavelength Thomson scattering (DLTS) technique presents a promising approach for precise measurements of electron temperatures, even at T_e values above which single wavelength spectral Thomson scattering loses precision because of the flattening of scattering profile [1]. For these reasons, such a technique is of particular interest in ITER where electron temperatures above 30keV are expected in the plasma core. Two laser pulses of different wavelengths are sent to the plasma with a very short time delay, and the two sets of signals are separately and independently measured with the same polychromator [2, 3]. Owing to the dependence of the TS spectrum from the input laser wavelength, the two sets of signals correspond to two different spectra, both related to the same T_e and n_e. The spectra of scattering signals collected in this way can be exploited either to 1) increase and extend the accuracy of the T_e and n_e measurements in the high T_e range or 2) determine and monitor the relative calibration factors of the polychromator spectral channels during the measurements (self-calibrating Thomson scattering).

In the past years, DLTS experiments have been performed on RFX using a 1053 nm Nd:YLF laser [4] and on LHD using a Ruby laser [5]. In both cases, the operation of the system was limited to a few measurement points. So far, a dual laser Thomson scattering based on the combination of a 1319 nm laser and 1064 nm laser as planned for ITER [6, 7] was never operated routinely during a plasma campaign.

Recently, a DLTS system was installed at W7-X with the purpose of testing the routine operation of such diagnostic. The W7-X DLTS system consists of three Nd:YAG lasers at 1064 nm wavelength with a maximum power output of 2.4 J at 30 Hz and a 1319 nm laser with a maximum energy output of 0.84 J per pulse at 10 Hz. The latter is combined with one of the 1064 nm laser before entering the torus hall using a beam combiner.The time delay between a 1064 nm laser pulse and a 1319 nm laser pulse is 50 µs. Note that the 1319 nm Nd:YAG laser is the first to reach a high energy output relevant to TS. Two collection optics, named inboard and outboard, are used [8]: the inboard system collects the scattered radiation with an angle ranging from 80 to 50 degrees, and the outboard system with an angle changing between 100 and 120 degrees. The polychromators have 5 channels,

collecting photons from 700 nm up to 1063 nm [8]. A detailed description of the DLTS system is provided by Pasch et al. [1].

In this work, the dual-wavelength signals recorded, during the last campaign OP2.1, in several W7-X discharges are analyzed and the electron temperature profiles and the experimental errors are discussed, with the aim of identifying the capabilities of this diagnostics.

2 Analysis of dual laser Thomson scattering signals

The objective of the analysis of Thomson scattering signals is to determine electron temperature and density, typically obtained by minimizing the residue between the measured and expected signal at a given electron temperature and density. In the specific case of W7-X DLTS, the focus is on improving the determination of the electron temperature extending the operational range of the diagnostic compared to a single laser system (here we do not consider a self-calibrating system). The way in which the chi-square function of the combination of the two spectra is written influences the final result.

The most straightforward way to write the χ^2 is as the sum of the single laser χ^2:

$$\chi^2 = \sum_i \frac{(X_i^{1064} - A^{1064} S_i^{1064}(T_e))^2}{\sigma_i^2} + \sum_j \frac{(Y_j^{1319} - A^{1319} S_j^{1319}(T_e))^2}{\sigma_j^2} \tag{2.1}$$

Where X_i and Y_j are the signals measured in the i_{th} and j_{th} polychromator channel and σ^2 the corresponding variance, $S_j^{1319}(T_e)$ and $S_i^{1064}(T_e)$ is the integration of the TS spectral density function in the jth and i^{th} polychromator channel as defined in [9]; A^{1064} and A^{1319} are determined from the fit and are equal to $n_e \Delta L \Delta\Omega \frac{\lambda_{\text{laser}} E_{\text{laser}}}{hc}$ [9], where ΔL is the scattering volume length and $\Delta\Omega$ the solid angle. eq. (2.1) leads to the determination of three independent parameters: an electron temperature and two parameters related to the electron density: A^{1064} and A^{1319}. Note that if the same polychromator (and the same channels) are used for acquiring the signals of the two lasers, $i = j$ in the sum. The main assumption in eq. (2.1) is that there is only one electron temperature.

The same equation can be modified under the assumption that the scattering volume crossed by the two lasers can be related by a factor γ:

$$\chi^2 = \sum_i \frac{(X_i^{1064} - A * S_i^{1064}(T_e))^2}{\sigma_i^2} + \sum_j \frac{(Y_j^{1319} - A * \gamma * S_j^{1319}(T_e))^2}{\sigma_j^2} \tag{2.2}$$

where A = A^{1064} and $\gamma = \frac{A^{1319}}{A^{1064}}$. In eq. (2.2) γ introduces a geometrical meaning to the ratio $\frac{A^{1319}}{A^{1064}}$, which allows to introduce of a constraint on the $\frac{A^{1319}}{A^{1064}}$ ratio in the fit. If the two laser beams are overlapping and have similar proprieties (pointing stability, divergence, and diameter etc.) γ can be considered only a function of the laser energy and wavelength $\gamma = \frac{\lambda_{1064} E_{1064}}{\lambda_{1319} E_{1319}}$, in this case, eq. (2.2) can be reduced to a two parameters fit (T_e and A), under the assumption that the scattering volume is exactly the same and the only difference between the intensity of the two signals is related to the number of photons in each laser pulse.

The measurement errors are the diagonal elements of the covariance matrix, which is related to the hessian of the χ^2 by the relation: C = $\frac{1}{2} H^{-1}$ [10]. In the case of eq. (2.2): with the 3 variables

T_e, A and γ the hessian is:

$$H = \begin{bmatrix} \frac{\partial^2 \chi^2}{\partial T_e^2} & \frac{\partial^2 \chi^2}{\partial T_e \partial A} & \frac{\partial^2 \chi^2}{\partial T_e \partial \gamma} \\ \frac{\partial^2 \chi^2}{\partial A \partial T_e} & \frac{\partial^2 \chi^2}{\partial A^2} & \frac{\partial^2 \chi^2}{\partial A \partial \gamma} \\ \frac{\partial^2 \chi^2}{\partial \gamma \partial T_e} & \frac{\partial^2 \chi^2}{\partial \gamma \partial A} & \frac{\partial^2 \chi^2}{\partial \gamma^2} \end{bmatrix} \tag{2.3}$$

In this work, the experimental errors are calculated using the exact analytic expression for the partial derivatives of the χ^2, which can be found in the appendix.

3 Operation of the DLTS system in OP 2.1
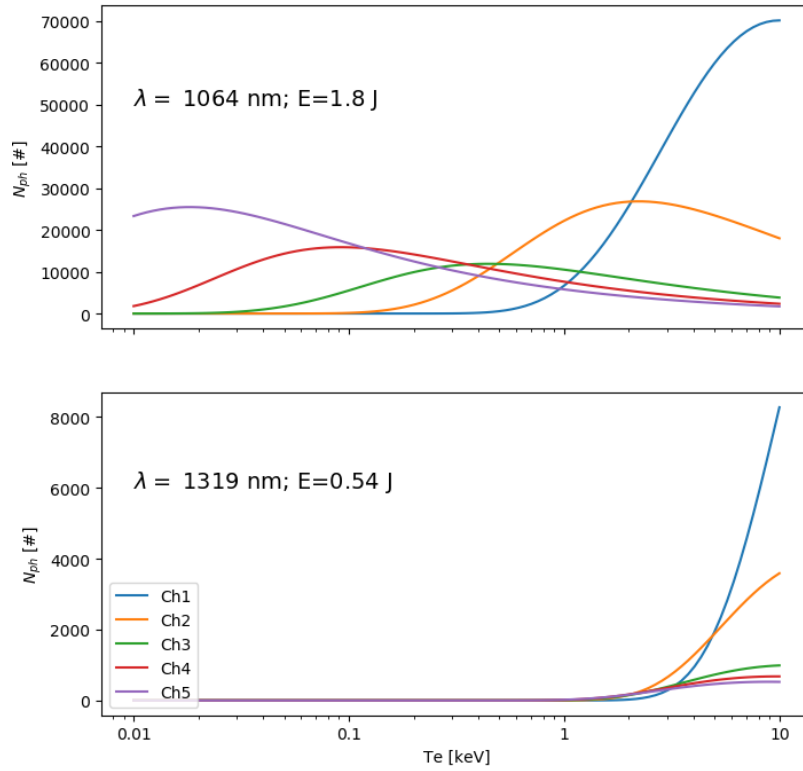
Figure 1. Expected signals at the core and at the edge of a discharge with low density ($5 \cdot 10^{19}$ m^{-3}) at the position measured from the outboard system.

The signal intensity of the DLTS system installed on W7-X is limited by the energy output of the longer wavelength laser and by the electron temperature that can be achieved in W7-X. Figure 1 shows the expected scattered photons from the two lasers as a function of the electron temperature at a scattering angle of 105°, corresponding to the core region measured by the outboard system, and a density of $5 \cdot 10^{19}$m^{-3}. The signals are simulated using a laser output energy of 1.8 J for the 1064 nm laser and 0.54 J for the 1319 nm laser. The signals from the secondary laser can be reliably measured only when the electron temperature rises above 2 keV. This limit is due to both the low
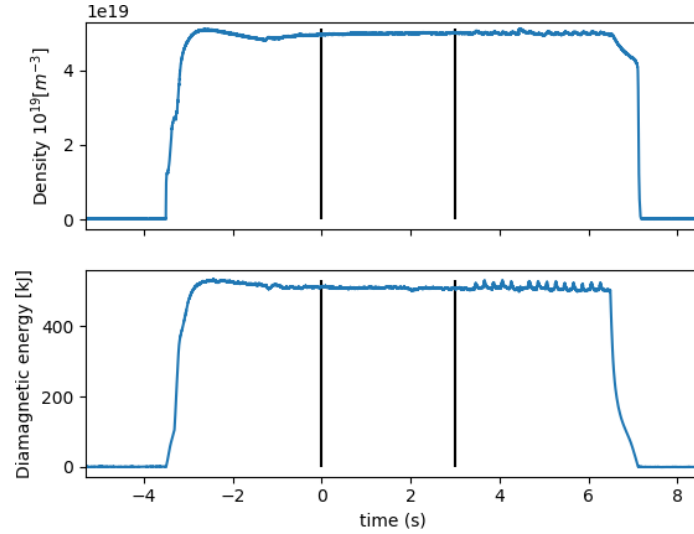
Figure 2. Line integrated density and diamagnetic energy for discharge 2230315.24. The vertical lines indicate the time in which the TS signals are average prior to analysis, t=0 is set at the beginning of the average window.

pulse energy of the 1319 nm laser and a suboptimal filter combination, which were selected to obtain the best electron temperature estimation with a single 1064 nm laser.

As a result, in W7-X discharges, single shot analysis is not possible as pointed out by Pasch et al. [1] and an average over several seconds is necessary. Moreover, the scattering signal broadening is maximized for the outboard system, where back scattered photons are measured [11]. Thus, the inboard system, which collects photons at scattering angles $< 70°$, measures signals from the 1319 nm laser only at temperatures above 3keV, in the discharge core.

As an example, the plasma discharge 20230315.24 is presented. This is a 10 s stable discharge with line integrated density of $5 \cdot 10^{19}$ m^{-3} and ECRH heating power of 4.4 MW and 1.8 MW of NBI heating. Figure 2 shows the time window considered for averaging. The standard deviation of the signals in this time window is used as an experimental error on the signals.

Figure 3 shows the signal recorded by polychromator P1, which is at the center of the discharge, on the left side the scattered signal for 1319 nm on the right side the scattered signals for 1064 nm. The signals are averaged in the time window shown in figure 2. Note that for the analysis, the signals are first fitted (within the W7-X analysis network [8]) and then averaged.

Figure 4 shows the electron temperature profiles obtained and the corresponding 2σ error bars. All plots show the temperature profile obtained by fitting the signals of the 1064 nm laser as the light blue area, which corresponds to the fitted $T_e \pm 2\sigma_{T_e}$. Figure 4(a) shows the temperature profile obtained by fitting the signals of the 1064 nm laser compared with the analysis of the signals of the 1319 nm laser. In this analysis, the signals are considered completely unrelated and analyzed separately. An electron temperature value can be obtained only for the scattering volumes observed with the outboard optics, and in which the electron temperature is above 2 keV. Despite the small energy per pulse of the 1319 nm laser it was possible to obtain an independent electron temperature value around the discharge core.
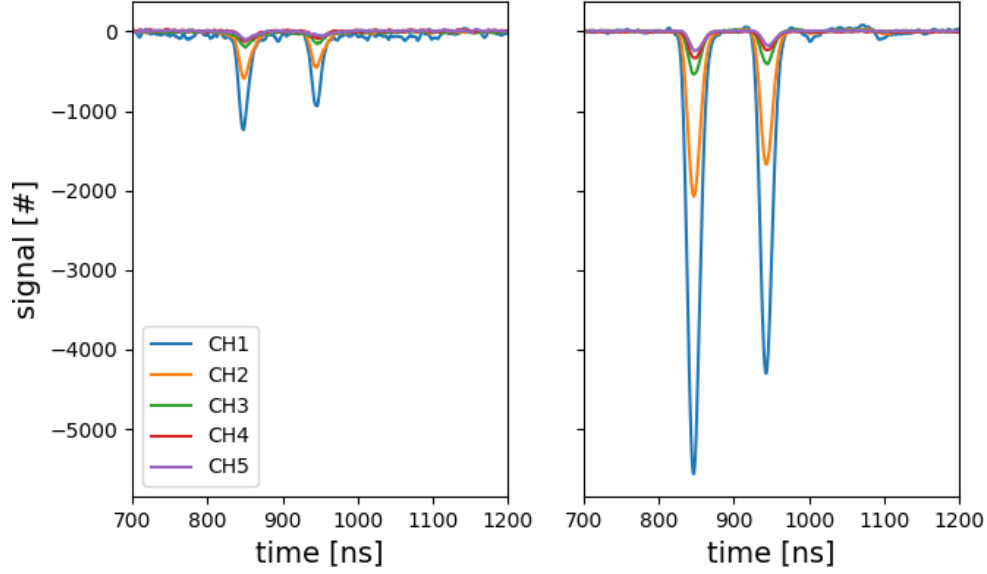
Figure 3. Thomson scattering signals measured in the core, by polychromator P1. On the left side, the TS signals from the 1319 nm, and on the right side the TS signals from the 1064 nm laser. The color code used for the different polychromator channels is the same one used in figure 1.

Figure 4(b) shows the temperature profile obtained by fitting both the 1064 and 1319 nm laser signals at the same time, imposing a single temperature with no restriction on the density parameters. Thus, minimizing the χ^2 function as written in eq. (2.1). The profile obtained in this way agrees well with the single laser analysis, with smaller error bars. Figure 4(c) shows the analysis performed minimizing the function (2.2), in this case, the parameter γ has been fitted assuming that it can be one hundred times smaller or one hundred times larger than its expected value $\sim \frac{\lambda_{1064} E_{1064}}{\lambda_{1319} E_{1319}}$. Note that if no boundaries are imposed, there is no difference between minimizing (2.1) and (2.2). Moreover, in most cases, γ does not converge properly, only in the discharge core, where the signal intensity from the 1319 nm laser is sufficient to properly determine the parameter. Also in this case the results show a good agreement with the single laser (1064 nm) analysis, although the γ parameter does not converge to its expected value (~ 0.4), but to a higher value ~ 0.8. Finally, figure 4(d) shows the result of minimizing eq. (2.2) while imposing a fixed γ parameter, in this case, it can be noted a systematic overestimation of the electron temperature, probably due to a systematic underestimation of the γ factor. It shall also be noted that the fit fails more often in the determination of T$_e$ when considering the signals of the 1319 nm, this is mainly related to the fact that the expected signals in these cases are small and affected by larger error. Whenever these errors are not evaluated correctly (e.g. systematic errors in determining zero signals) the fit may converge to a spurious value.

The errors in the determination of the fitting parameters can be determined according to eq. (2.3). Theoretically, the errors should weakly improve for the scattering volumes near the plasma core, where there are signals from the 1319 nm laser. Figure 5 shows the ratio between σ_{TS}, the error on the electron temperature obtained in a single laser fit, and σ_{DLTS}, the error on the electron temperature determined with dual laser fit. It should be noted that in several cases it is not possible to obtain analytically a valid error, this is due to the fact that the curvature matrix has a dependence on the difference between the measured signal and the experimental signal. This should be close to zero,
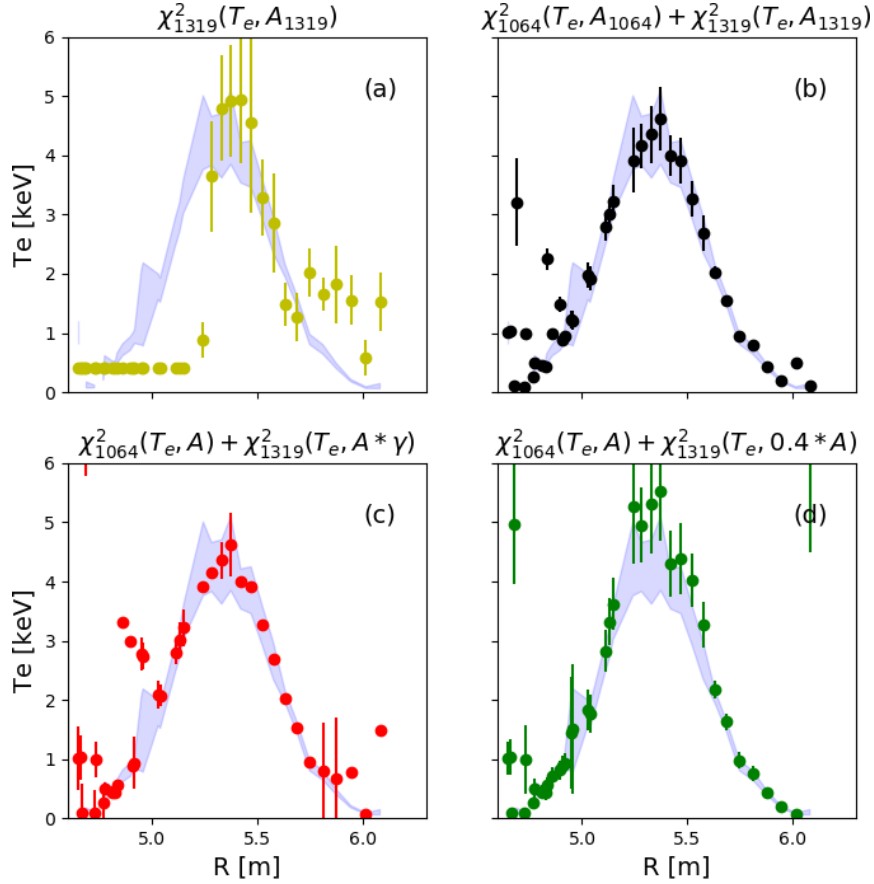
Figure 4. Electron temperature profiles measured in discharge 2 0230315.24. The blue shadow represents the electron temperature calculated using the signal of the 1064 nm laser compared with the electron temperature calculated using only the signal from the 1319 nm laser (plot (a), yellow dots), both signals making no assumption on the scattering volume (plot (b), black dots), both signals assuming the same scattering volume is measured by the two lasers with an experimental error (plot (c), red dots), both signals assuming the ratio of the laser's photons within a scattering volume is fixed (plot (d), green d ots). The error bars shown correspond to 2σ.

but for channels in which large deviations from their expected values occur, its contribution can become dominant. In these cases, the inverse of the Hessian has negative values on the diagonal, resulting in an imaginary standard deviation. This means there is no minimum, which is normal for not converged fits and for fits with bo undaries. Such problems occur mostly in figure 5(a), in the region R < 5.3 m for those points where the analysis did not converge and in figure 5(c), in the region of 5.3 m < R < 5.8 m, where the boundaries on the γ parameter can lead to a large deviation between measured and fit scattering signals produced by the secondary 1319 nm laser. An improvement in the determination of the electron temperature is observed consistently only in figure 5(b), where the p arameter A_{1319} can change freely and match better the experimental signals.

The improvement obtained on the error determination is limited to $\sim 20\%$, and it is limited to near the core of the discharge. The improvement is limited because of the low pulse energy of the 1319 nm laser. The observed improvement is comparable to the expectations [12].
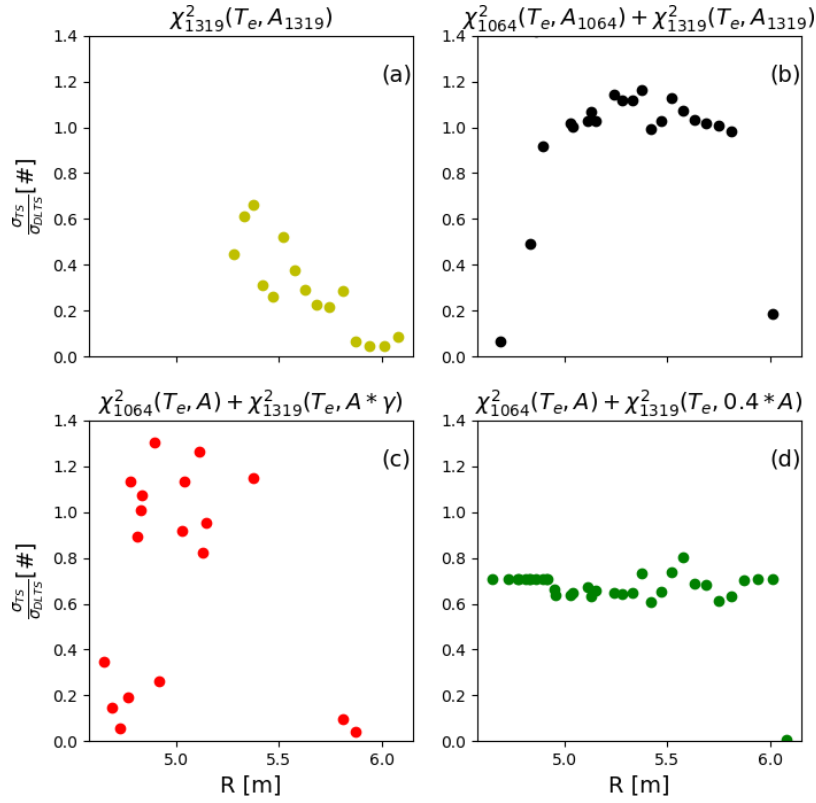
Figure 5. The ratio between the error bars of the electron temperature, as shown in figure 4. σ_{TS} is the error on the electron temperature obtained in a single laser fit, while σ_{DLTS} is the error on the electron temperature determined with dual laser fit.

The W7-X DLTS represents a first of a kind, the continuous operation of such a system during W7-X OP2.1 campaign has proven the reliability of the system, albeit identifying that the pointing stability of the 1319 nm laser during the operation was not optimized. Additional research and development is required to demonstrate the functionality of a more powerful 1319 nm laser, such a laser will not only allow to perform single-shot analysis but also test the possibilities of the self-calibration technique, which in the W7-X setup it is not possible at the moment because of lack of signal intensity.

4   Conclusion

In this paper, the first signals of a dual laser Thomson scattering system employing a 1319 nm laser are analyzed using several approaches. The capabilities of the system are limited by the energy per pulse of the 1319 nm laser, the geometry of the acquisition optics, and the polychromator configuration. All these factors imply the necessity to average the signals to obtain data that can be analyzed. Electron temperature profiles could be obtained using different minimization approaches, in the best case an improvement of 20% in the determination of the electron temperature could be obtained.

Acknowledgments

A Derivatives of $\chi^2(T_e, A, \gamma)$

The derivatives are shown in eq. (2.3) are:

$$\frac{\partial^2 \chi^2}{\partial T_e^2} = \sum_i \left[\frac{2 * A^2 * (S_i'^{1064})^2}{\sigma_i^2} - \frac{2 * A * S_i''^{1064} * (X_i - A * S_i^{1064}(T_e))}{\sigma_i^2} \right]$$
$$+ \sum_j \left[\frac{2 * A^2 * (S_j'^{1319})^2 * \gamma^2}{\sigma_j^2} - \frac{2 * A * S_j''^{1319} * \gamma * (Y_j - A * \gamma * S_j^{1319}(T_e))}{\sigma_j^2} \right] \tag{A.1}$$

$$\frac{\partial^2 \chi^2}{\partial A^2} = \sum_i \left[\frac{2 * S_i^{1064}(T_e)^2}{\sigma_i^2} \right] + \sum_j \left[\frac{2 * \gamma^2 * S_j^{1319}(T_e)^2}{\sigma_j^2} \right] \tag{A.2}$$

$$\frac{\partial^2 \chi^2}{\partial \gamma^2} = \sum_j \left[\frac{2 * A^2 * S_j^{1319}(T_e)^2}{\sigma_j^2} \right] \tag{A.3}$$

$$\frac{\partial^2 \chi^2}{\partial T_e \partial A} = \sum_i \left[\frac{2 * A * S_i'^{1064} * S_i^{1064}(T_e)}{\sigma_i^2} - \frac{2 * S_i'^{1064} * (-A * S_i^{1064}(T_e) + X_i)}{\sigma_i^2} \right]$$
$$+ \sum_j \left[\frac{2 * A * S_j'^{1319} * \gamma^2 * S_j^{1319}(T_e)}{\sigma_j^2} - \frac{2 * S_j'^{1319} * \gamma * (-A * \gamma * S_j^{1319}(T_e) + Y_j)}{\sigma_j^2} \right] \tag{A.4}$$

where S' and S" are the derivatives of the spectral photon density after the derivation of the expressions given in [11].

References

[1] E. Pasch, M.N.A. Beurskens, S.A. Bozhenkov, G. Fuchert and R.C. Wolf and the W7-X Team, *Dual-laser wavelength thomson scattering at wendelstein 7-x*, *Rev. Sci. Instrum.* **89** (2018) 10C115.

[2] L. Giudicotti and R. Pasqualotto, *Dual-laser calibration of thomson scattering systems in ITER and RFX-mod*, *Nucl. Fusion* **54** (2014) 043005.

[3] O.R.P. Smith, C. Gowers, P. Nielsen and H. Salzmann, *A self-calibration technique for a thomson scattering system*, *Rev. Sci. Instrum.* **68** (1997) 725.

[4] O. McCormack, L. Giudicotti, A. Fassina and R. Pasqualotto, *Dual-laser, self-calibrating thomson scattering measurements in RFX-mod*, *Plasma Phys. Control. Fusion* **59** (2017) 055021.

[5] E. Yatsuka, *Dual-laser self-calibrating Thomson scattering experiments in LHD*, submitted to *JINST* (2023).

[6] M. Bassan et al., *Thomson scattering diagnostic systems in ITER*, 2016 *JINST* **11** C01052.

[7] R. Scannell et al., *Design advances of the core plasma thomson scattering diagnostic for ITER*, 2017 *JINST* **12** C11010.

[8] E. Pasch et al., *The Thomson scattering system at Wendelstein 7-X*, *Rev. Sci. Instrum.* **87** (2016) 11E729.

[9] O. Naito, H. Yoshida, S. Kitamura, T. Sakuma and Y. Onose, *How many wavelength channels do we need in thomson scattering diagnostics?*, *Rev. Sci. Instrum.* **70** (1999) 3780.

[10] S. Brandt and M. Alexanian, *Statistical and computational methods in data analysis*, *Am. J. Phys.* **39** (1971) 1109.

[11] S.L. Prunty, *A primer on the theory of Thomson scattering for high-temperature fusion plasmas*, *Phys. Scripta* **89** (2014) 128001.

[12] L. Giudicotti, *2021-W7X-5.2.1-ENEA-RFX: Report on the development of dual-laser and dual-angle Thomson scattering*, resreport WPTX — Eurofusion (2021).